Oxidations of *p*-Alkoxyacylanilides Catalyzed by Human Cytochrome P450 1A2: Structure−Activity Relationships and Simulation of Rate Constants of Individual Steps in Catalysis†

Chul-Ho Yun,‡ Grover P. Miller, and F. Peter Guengerich*

Department of Biochemistry and Center in Molecular Toxicology, Vanderbilt University School of Medicine, Nashville, Tennessee 37232-0146

Received December 21, 2000; Revised Manuscript Received February 1, 2001

ABSTRACT: Human cytochrome P450 (P450) 1A2 is involved in the oxidation of many important drugs and carcinogens. The prototype substrate phenacetin is oxidized to an acetol as well as the *O*-dealkylation product [Yun, C.-H., Miller, G. P., and Guengerich, F. P. (2000) *Biochemistry 39*, 11319−11329]. In an effort to improve rates of catalysis of P450 1A2 enzymes, we considered a set of *p*-alkoxyacylanilide analogues of phenacetin and found that variations in the *O*-alkyl and *N*-acyl substituents altered the rates of the two oxidation reactions and the ratio of acetol/phenol products. Moving one methylene group of phenacetin from the *O*-alkyl group to the *N*-acyl moiety increased rates of both oxidations ∼5-fold and improved the coupling efficiency (oxidation products formed/NADPH consumed) from 6% to 38%. Noncompetitive kinetic deuterium isotope effects of 2−3 were measured for all *O*-dealkylation reactions examined with wild-type P450 1A2 and the E225I mutant, which has 6-fold higher activity. A trend of decreasing kinetic deuterium isotope effect for E225I > wild-type > mutant D320A was observed for *O*-demethylation of *p*-methoxyacetanilide, which follows the trend for k_{cat}. The set of *O*-dealkylation and acetol formation results for wild-type P450 1A2 and the E225I mutant with several of the protiated and deuterated substrates were fit to a model developed for the basic catalytic cycle and a set of microscopic rate constants in which the only variable was the rate of product formation (substrate oxygenation, including hydrogen abstraction). In this model, k_{cat} is considerably less than any of the microscopic rate constants and is affected by several individual rate constants, including the rate of formation of the oxygenating species, the rate of substrate oxidation by the oxygenating species, and the rates of generation of reduced oxygen species (H_2O_2, H_2O). This analysis of the effects of the individual rate constants provides a framework for consideration of other P450 reactions and rate-limiting steps.

The microsomal P450s[1] are the major enzymes involved in the oxidation of xenobiotic chemicals in eukaryotes (*4*, *5*). The great majority of these reactions are mixed-function oxidations (monooxygenations). The general consensus is that high valent iron−oxygen species (e.g., FeO^{3+}) are involved in the actual substrate oxidation (*6*−*10*). Although a few general catalytic mechanisms appear to be operative for most of the reactions catalyzed by the P450s (*4*), certain features such as rate-limiting steps and substrate interactions may vary considerably depending on the particular P450 and the reaction involved (*11*).

Scheme 1: General Mechanism of P450 Catalysis[a]

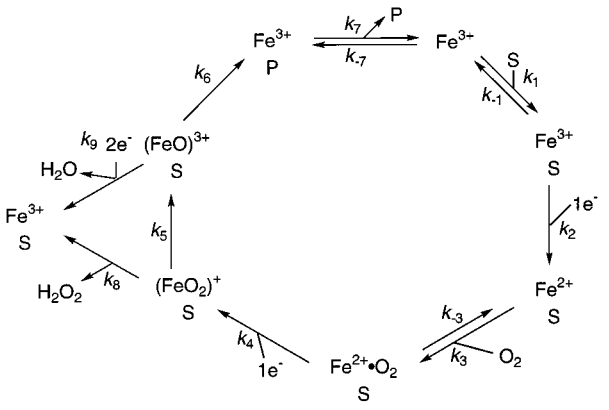

[a] References *4*, *6*, and *12*. This scheme is developed later in the kinetic simulations.

Possible rate-limiting steps in P450 catalysis (Scheme 1) include substrate binding (k_1), reduction (k_2), oxygen binding to ferrous P450 (k_3), addition of the second electron to the system (k_4), rearrangement to the final active oxygen species (k_5), C−H bond cleavage in the substrate (part of k_6), and product release (k_7). The issue of rate-limiting steps in P450 reactions has been considered many times (*6*). In general,

† This work was supported by U.S. Public Health Service (USPHS) Grants R35 CA44353 and P30 ES00267. G.P.M. was supported in part by USPHS postdoctoral fellowship F32 GM19808.

* To whom correspondence should be addressed: Department of Biochemistry and Center in Molecular Toxicology, Vanderbilt University School of Medicine, 638 Medical Research Building I, 23rd and Pierce Ave., Nashville, TN 37232-0146. Tel: 615-322-2261. Fax: 615-322-3141. E-mail: guengerich@toxicology.mc.vanderbilt.edu.

‡ Present address: Department of Genetic Engineering, Pai-Chai University, Taejon 302−735, South Korea.

[1] Abbreviations: P450, cytochrome P450 [also termed heme-thiolate P450 by the Enzyme Commission (EC 1.14.14.1) (*1*)]; MS, mass spectrometry. The conventions used for the kinetic deuterium isotope effects are those of Northrop (*2*, *3*): $^{D}V = {}^{H}k_{cat}/{}^{D}k_{cat}$, $^{D}(V/K) = ({}^{H}k_{cat}/{}^{H}K_m)/({}^{D}k_{cat}/{}^{D}K_m)$, and ^{D}k = intrinsic isotope effect on a reaction step.

10.1021/bi002906n CCC: $20.00
Published on Web 03/16/2001

Table 1: Substrates and Products

	R_1	R_2	chemical name
substrates			
phenacetin	CH_2CH_3	CH_3	*N*-(4-ethoxyphenyl)acetamide
1 (methacetin)	CH_3	CH_3	*N*-(4-methoxyphenyl)acetamide
2	$CH(CH_3)_2$	CH_3	*N*-[4-(1-methylethoxy)phenyl]acetamide
3	CH_2CH_3	CH_2CH_3	*N*-(4-ethoxyphenyl)propionamide
4	CH_3	CH_2CH_3	*N*-(4-methoxyphenyl)propionamide
5	CH_2CH_3	$CH(CH_3)_2$	*N*-(4-ethoxyphenyl)isobutyramide
products			
6	H	CH_3	*N*-(4-hydroxyphenyl)acetamide
7	H	CH_2CH_3	*N*-(4-hydroxyphenyl)propionamide
8	H	$CH(CH_3)_2$	*N*-(4-hydroxyphenyl)isobutyramide
9	CH_3	CH_2OH	*N*-(4-methoxyphenyl)hydroxyacetamide
10	CH_2CH_3	CH_2OH	*N*-(4-ethoxyphenyl)hydroxyacetamide
11	$CH(CH_3)_2$	CH_2OH	*N*-[4-(1-methylethoxy)phenyl]hydroxyacetamide
12	CH_2CH_3	$CH(OH)CH_3$	*N*-(4-ethoxyphenyl)-2-hydroxypropionamide
13	CH_3	$CH(OH)CH_3$	*N*-(4-methoxyphenyl)-2-hydroxypropionamide
14	CH_2CH_3	$CH(CH_3)_2OH$	*N*-(4-ethoxyphenyl)-2-hydroxyisobutyrpropionamide
15	$CH(CH_3)CH_2OH$	CH_3	*N*-[4-(1-hydroxymethylethoxy)phenyl]acetamide

most investigators have considered the introduction of the first (k_2) or second electron (k_4) into the system to be the rate-limiting step. These views are based primarily on the low concentration of NADPH−P450 reductase in microsomes and the slow rates of ferric P450 reduction observed in the absence of substrate (*11*, *13*). However, many P450s are reduced rapidly, including P450 1A2 (*11*). The view that the rate of input of the second electron into the system (Scheme 1, k_4) is rate-limiting is based primarily on the observed stimulation of some reactions by cytochrome b_5, electron transfer from which is postulated to be more kinetically more favorable in some instances (*6*, *14*−*16*). Kinetic hydrogen isotope effects have been measured in P450 reactions as a means toward elucidation of rate-limiting steps. The general view with the reactions examined has been that intrinsic hydrogen isotope effects, associated with C−H cleavage, are high [and have been used as evidence for a hydrogen abstraction mechanism (*7*−*9*, *17*)] but that noncompetitive isotope effects are low (*7*, *9*, *18*), with some exceptions (*19*−*21*).

Phenacetin is a prototypic substrate of human P450 1A2, an enzyme first characterized as the major phenacetin *O*-deethylase (*22*, *23*). P450 1A2 catalyzes the activation of numerous potentially carcinogenic aryl and heterocyclic amines (*23*, *24*) and is expressed essentially only in liver. Some major species differences in catalytic activity of P450 1A2 enzymes have been characterized (*25*). Recently, we selected P450 1A2 mutants with altered activity in a random mutagenesis approach using mutated "substrate recognition site" regions (*26*), including some with enhanced activity due to substitution of a single residue (*27*).

Wild-type P450 1A2 shows only 6% coupling efficiency for phenacetin oxidation (ratio of product formed/NADPH oxidized) (*12*). Kinetic studies on rate-limiting steps in phenacetin *O*-deethylation (*12*) and other mechanistic studies with P450 1A2 enzymes (*28*−*30*) are compromised by the low rates and coupling efficiency. In this work, we systematically examined a series of *p*-alkoxyacylanilide compounds to find higher oxidation rates of *O*-dealkylation and *N*-acyl group hydroxylation (acetol formation, Scheme 2) by P450 1A2 wild-type and mutant enzymes (Table 1). Steady-state kinetic parameters (k_{cat} and K_m) and kinetic deuterium isotope effects were determined. Within the set of substrates used,

Scheme 2: Oxidations of *p*-Alkoxyacylanilides by P450 1A2[a]

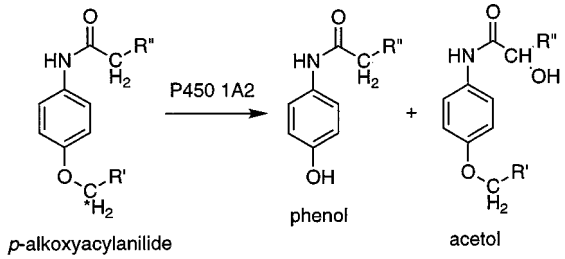

[a] The site of deuterium substitution utilized in kinetic experiments is labeled with an asterisk.

rates (k_{cat}) of *O*-dealkylation varied 25-fold and rates of acetol formation varied 120-fold. Comparisons allow inference into structural features that facilitate oxidation. The steady-state results provided an extensive data set for kinetic modeling of the P450 1A2 catalytic cycle, which could be done in a system approximating the most generally accepted catalytic cycle (Scheme 1) and limited by several experimental steady-state and pre-steady-state rates (*12*). The contributions of rates of individual steps in the catalytic cycle to the steady-state k_{cat} and K_m are considered.

EXPERIMENTAL PROCEDURES

Chemicals. Acetaminophen, 4-aminophenol, and all deuterated reagents were obtained from Aldrich Chemical Co. (Milwaukee, WI). Methacetin (**1**, Table 1) was obtained from ACROS (Pittsburgh, PA). Other chemicals were of the highest grade commercially available.

Syntheses of Substrates and Products. *p*-Alkoxyacylanilides used in this study were usually prepared by either of two general procedures: (i) from the *p*-hydroxyacylanilides and appropriate haloalkane (*31*); (ii) from the *p*-alkoxyanilines and corresponding acids (or acid anhydrides) (*12*, *32*). Yields were in the range of 60−90% (for crystalline products). All melting points were determined with a Mel-Temp apparatus (Laboratory Devices, Cambridge, MA) and are uncorrected. Elemental analyses were done by Galbraith Laboratories (Knoxville, TN).

N-(4-[1,1,1-^{2}H]Methoxyphenyl)acetamide (d_3-methacetin) (**1**) was prepared from compound **6** (Table 1) and C^2H_3I as described (*33*) and recrystallized twice from CH_3OH/H_2O

(mp 131−133 °C; manufacturer's mp of protiated material listed as 128−130 °C). Mass spectra yielded the expected molecular ions (MH^+) for the protiated (Aldrich) (*m*/*z* 166) and deuterated compounds (*m*/*z* 169), and the ^{1}H NMR spectrum of deuterium-labeled methacetin differed from that of the unlabeled compound only in the lack of the corresponding protons (δ 3.72), ≥99% isotopic abundance.

N-[4-(1-Methylethoxy)phenyl]acetamide (**2**) was synthesized from compound **6** and 2-iodopropane (*31*, *33*) and recrystallized twice from CH_3OH/H_2O: mp 130−131 °C [lit. 130−131 °C (*34*)]; *m*/*z* 194 (MH^+); ^{1}H NMR ($CDCl_3$) δ 1.24 [d, 6H, $CH(CH_3)_2$], 2.06 (s, 3H, $COCH_3$), 4.40 [m, 1H, $CH(CH_3)_2$], 6.76−7.18 (m, 5H, ArH).

N-(4-Ethoxyphenyl)propionamide (**3**) was prepared from *p*-phenetidine and propionic anhydride (*35*, *36*) and recrystallized from CH_3OH/H_2O: mp 117−118 °C [lit. 120 °C (*35*)]; *m*/*z* 194 (MH^+); ^{1}H NMR ($CDCl_3$) δ 1.26 (t, 3H, $-COCH_2CH_3$), 1.41 (t, 3H, $-OCH_2CH_3$), 2.38 (q, 2H, $COCH_2CH_3$), 4.02 (q, 2H, $-OCH_2CH_3$), 6.86−7.41 (m, 5H, ArH).

N-(4-Ethoxyphenyl)[2,2-^{2}H]propionamide (d_2-**3**) was synthesized from *p*-phenetidine and [2,2-^{2}H]propionic acid (Aldrich). Mass spectra yielded the expected molecular ions for the protiated (*m*/*z* 194, MH^+) and deuterated (*m*/*z* 196, MH^+) compounds, and the ^{1}H NMR spectrum of the deuterium-labeled compound differed from that of the unlabeled compound only by the lack of the corresponding protons (δ 2.38), ≥99% isotopic abundance.

N-(4-Methoxyphenyl)propanamide (**4**) was prepared from *p*-anisidine and propionic anhydride and recrystallized from CH_3OH/H_2O: mp 83−84 °C [lit. 89−91 °C (*37*)];[2] *m*/*z* 180 (MH^+); ^{1}H NMR ($CDCl_3$) δ 1.17 (t, 3H, $COCH_2CH_3$), 2.30 (q, 2H, $COCH_2CH_3$), 3.72 (s, 3H, OCH_3), 6.78−7.34 (m, 5H, ArH).

N-(4-Ethoxyphenyl)-2-methylpropionamide (**5**) was synthesized from compound **8** and C_2H_5I (*40*) and recrystallized twice from CH_3OH/H_2O: mp 133−134 °C [lit. 134 °C (*40*)]; *m*/*z* 208 (MH^+); ^{1}H NMR ($CDCl_3$) δ 1.26 [t, 6H, $COCH(CH_3)_2$], 1.41 (t, 3H, $-OCH_2CH_3$), 2.38 (q, 1H, $COCH_2CH_3$), 4.02 (q, 2H, $-OCH_2CH_3$), 6.86−7.41 (m, 5H, ArH).

N-(4-Hydroxyphenyl)propionamide (**7**) was prepared from 4-aminophenol and propionic anhydride and recrystallized from C_2H_5OH/H_2O: mp 169−170 °C [lit. 167−168 °C (*37*)]; *m*/*z* 166 (MH^+); ^{1}H NMR (CD_3OD) δ 1.14 (t, 3H, CH_2CH_3), 2.28 (q, 2H, CH_2CH_3), 6.67−7.25 (m, 5H, ArH).

N-(4-Hydroxyphenyl)-2-methylpropionamide (**8**) was prepared from 4-aminophenol and isobutyric anhydride and recrystallized from C_2H_5OH/H_2O: mp 163−164 °C [lit. 164 ° C (*41*, *42*)]; *m*/*z* 180 (MH^+); ^{1}H NMR (CD_3OD) δ 1.20 [d, 6H, $CH(CH_3)_2$], 2.60 [m, 1H, $CH(CH_3)_2$], 6.75−7.33 (m, 5H, ArH).

N-(4-Methoxyphenyl)hydroxyacetamide (**9**), the acetol product derived by hydroxylation of methacetin, was synthesized (*32*) and recrystallized twice from ethyl acetate: mp 98−99 °C [lit. 95−96 °C (*32*)]; *m*/*z* 182 (MH^+); ^{1}H NMR ($CDCl_3$) δ 3.72 (s, 3H, $-OCH_3$), 4.16 (s, 2H, CCH_2OH), 6.79−7.39 (m, 5H, ArH), 8.08 (br, 1H, NH).

N-[4-(1-Methylethoxy)phenyl]hydroxyacetamide (**11**)[3] was prepared from *N*-(4-hydroxyphenyl)hydroxyacetamide (vide infra) and 2-iodopropane and recrystallized from CH_3OH/H_2O: mp 78−79 °C; *m*/*z* 210 (MH^+); ^{1}H NMR (d_6-dimethyl sulfoxide) δ 1.41 [d, 6H, $CH(CH_3)_2$], 4.10 (s, 2H, $COCH_2OH$), 4.71 [m, 1H, $CH(CH_3)_2$], 5.81 (br, 1H, OH), 7.01−7.74 (m, 5H, ArH), 9.67 (br, 1H, NH). Elemental analysis: calculated for $C_{11}H_{15}NO_3$, C 63.16, H 7.18, N 6.70; found, C 62.79, H 7.23, N 6.58. *N*-(4-Hydroxyphenyl)hydroxyacetamide was prepared from *p*-aminophenol and glycolic acid as described (*43*) and recrystallized from H_2O: mp 138−139 °C; *m*/*z* 168 (MH^+); ^{1}H NMR (d_6-dimethyl sulfoxide) δ 3.93 (s, 2H, $COCH_2OH$), 5.59 (br, 1H, OH), 6.68−7.44 (m, 5H, ArH), 9.27 (br, 1H, NH).

N-(4-Ethoxyphenyl)-2-hydroxypropionamide (**12**) was synthesized from *p*-phenetidine and lactic acid (*32*) and recrystallized twice from CH_3OH/H_2O: mp 149−150 °C [lit. 106.5 °C (*44*) and 118 °C (*45*)];[4] *m*/*z* 210 (MH^+); ^{1}H NMR ($CDCl_3$) δ 1.18 (t, 3H, CH_2CH_3), 1.30 [d, 3H, $COCH(OH)CH_3$], 3.79 (q, 2H, CH_2CH_3), 4.14 [q, 1H, $COCH(OH)CH_3$], 6.63−7.23 (m, 5H, ArH), 8.28 (br, 1H, NH).

N-(4-Methoxyphenyl)-2-hydroxypropionamide (**13**) was synthesized from *p*-anisidine and lactic acid (*44*) and recrystallized twice from CH_3OH/H_2O: mp 105−106 °C [lit. 79−80 °C (*44*)];[5] *m*/*z* 196 (MH^+); ^{1}H NMR ($CDCl_3$) δ 1.49 [d, 3H, $COCH(OH)CH_3$], 3.75 (s, 3H, $-OCH_3$), 4.32 [q, 1H, $COCH(OH)CH_3$], 6.80−7.41 (m, 5H, ArH), 8.19 (br, 1H, NH).

N-(4-Ethoxyphenyl)-2-hydroxy-2-methylpropionamide (**14**) was prepared from *p*-phenetidine and 2-hydroxyisobutyric acid (*32*) and recrystallized twice from CH_3OH/H_2O: mp 149−150 °C [lit. 146−148 °C (*46*)]; *m*/*z* 224 (MH^+); ^{1}H NMR (d_6-dimethyl sulfoxide) δ 1.50 (t, 3H, CH_2CH_3), 1.53 [s, 6H, $COC(CH_3)_2OH$], 4.17 (q, 2H, CH_2CH_3), 5.84 (br, 1H, OH), 7.04−7.80 (m, 5H, ArH), 9.58 (br, 1H, NH).

N-[4-(1-Hydroxymethylethoxy)phenyl]acetamide (**15**) was synthesized from **6** and 2-chloro-1-propanol: *m*/*z* 210 (MH^+); ^{1}H NMR (d_6-dimethyl sulfoxide) δ 1.04 [d, 3H, $CH(CH_2OH)CH_3$], 1.91 (s, 3H, $COCH_3$), 3.65 [m, 2H, $CH(CH_2OH)CH_3$], 3.81 [m, 1H, $CH(CH_2OH)CH_3$], 4.72 (br, 1H, OH), 6.77−7.37 (m, 5H, ArH), 9.65 (br, 1H, NH).

Expression and Purification of Recombinant Wild-Type P450 1A2 and Mutants. Recombinant P450 1A2 enzymes containing a C-terminal $(His)_5$ tag were prepared from a P450 1A2 construct (containing a modification of the N-terminus) (*27*, *47*). Expression of P450 1A2 enzymes with C-terminal $(His)_5$ tags in *Escherichia coli* DH5α was accomplished as described earlier, and *E. coli* membranes were prepared (*47*) and used as a source for the purification of P450s by Ni^{2+}-nitrilotriacetate chromatography (*12*).

Spectroscopy. UV−vis spectra were recorded using an Amino DW2a/OLIS instrument (On-Line Instrument Systems, Bogart, GA). Fluorescence titrations were done with an SPEX Fluorolog spectrophotomer (SPEX, Edison, NJ) utilizing P450 1A2 tryptophan fluorescence, as described previously in detail (*12*). ^{1}H NMR spectra were recorded on

[2] Another preparation yielded crystals with mp 117−118 °C, which also has literature precedent [mp 120.5−122.5 °C (*38*, *39*)]. The spectral properties (MS, ^{1}H NMR) were identical and verify the structure.

[3] Not found in *Chemical Abstracts* or *Beilstein*. The precursor phenol is CA Registry No. 54704-27-7.

[4] Although the melting point differs from the literature (considerably higher than either literature value), the spectral properties leave no doubt that this is the expected product.

[5] Mp 106.5 °C in German Patent DE 70250.

Table 2: Kinetic Parameters of Oxidation of *p*-Alkoxyacylanilides by P450 1A2

			O-dealkylation		*C*-hydroxylation	
substrate	R_1	R_2	k_{cat} (min^{-1})	K_m (μM)	k_{cat} (min^{-1})	K_m (μM)
1 (methacetin)	CH_3	CH_3	2.7 ± 0.1	28 ± 3	0.039 ± 0.010	20 ± 7
phenacetin	CH_2CH_3	CH_3	1.8 ± 0.1	16 ± 1	0.35 ± 0.01	17 ± 2
2	$CH(CH_3)_2$	CH_3	0.43 ± 0.02	90 ± 12	0.16 ± 0.01	36 ± 8
3	CH_2CH_3	CH_2CH_3	8.0 ± 0.5	140 ± 20	4.9 ± 0.3	130 ± 20
4	CH_3	CH_2CH_3	11 ± 1	14 ± 2	2.0 ± 0.2	130 ± 20
5	CH_2CH_3	$CH(CH_3)_2$	7.4 ± 0.3	180 ± 20	2.5 ± 0.1	380 ± 30

a Bruker AM 400 spectrometer operating at 400.13 MHz and 27 °C (Bruker, Billerica, MA) in the Vanderbilt facility. Samples were prepared in $CDCl_3$, CD_3OD, or d_6-dimethyl sulfoxide (100.0 atom % D grade, Aldrich). Mass spectrometry was done with a HP 5890A gas chromatograph (Hewlett-Packard Co., Wilmington, DE) linked to a Finnigan MAT INCOS 50 mass spectrometer (Finnigan MAT, San Jose, CA) unless noted otherwise (positive ion mode).

Catalytic Activity Assays. *p*-Alkoxyacylanilide *O*-dealkylation and acetol formation activities were determined by HPLC of the reaction products (*48*), with slight modification in the kinetic hydrogen isotope effect studies.

P450 reaction mixtures included 0.40 μM P450 1A2, 0.80 μM NADPH−P450 reductase (purified recombinant rat enzyme expressed in *E. coli*) (*49*, *50*), L-α-dilauroyl-*sn*-glycero-3-phosphocholine (45 μM), 100 mM potassium phosphate buffer (pH 7.4), an NADPH-generating system [0.50 mM $NADP^+$, 10 mM glucose 6-phosphate, and 1.0 IU of glucose-6-phosphate dehydrogenase mL^{-1} (*51*)], and varying concentrations of substrate (2.0−200 μM *p*-alkoxyacylanilide) in a total volume of 0.50 mL. Incubations were generally done for 10 min at 37 °C, terminated with 0.10 mL of 17% $HClO_4$, and centrifuged (10^3g, 10 min). A mixture of $CHCl_3$ and 2-propanol (1.0 mL, 6:4 v/v) was added to the supernatant to extract the products, followed by centrifugation (twice at 10^3g). The organic layers were combined, and solvent was removed under N_2 (at room temperature). The products (phenols and acetols) were analyzed by HPLC using a Beckman Ultrasphere C_{18} column (4.6 × 250 mm, 5 μm) with the mobile phase H_2O:CH_3OH:CH_3CO_2H (65:35:0.1 v/v/v), flow rate 1.0 mL min^{-1}, monitoring A_{254}. Kinetic parameters (K_m and k_{cat}) were determined using nonlinear regression with Graph-Pad Prism software (San Diego, CA).

Estimation of Kinetic Isotope Effects. Deuterium isotope effects were determined by both noncompetitive and competitive methods (*2*, *3*). In the noncompetitive experiments, P450 1A2 was incubated with either the unlabeled (d_0) or labeled (d_2, d_3, or d_7 at site of oxidation) *p*-alkoxyacylanilide using a range of substrate concentrations (2.0−200 μM), and the products were analyzed by HPLC as described. K_m and k_{cat} were estimated by nonlinear regression analysis as described above.

Two competitive approaches were also used to measure deuterium isotope effects. (i) P450 1A2 was incubated with a 1:1 molar mixture of unlabeled (d_0) and substrate-labeled in the methoxy group (d_3) (**1** or **4**, final concentration 200 μM), and the resulting formaldehyde was extracted and analyzed by combined GC/MS (positive ion electron impact) following derivatization with 2,4-dinitrophenylhydrazine (*52*). The hydrazone derivatives were analyzed as described (*53*), with separation on a 15-m SPB-1 fused silica capillary column (Supelco, Bellefonte, PA) interfaced to a Hewlett-Packard 5890 mass spectrometer (Hewlett-Packard, Palo Alto, CA). Conditions were as follows: injection port 230 °C, transfer line 260 °C, and initial column temperature 100 °C increased to 320 °C at a rate of 25 °C min^{-1}. The [^{1}H]-formaldehyde hydrazone was detected by selected ion monitoring at *m*/*z* 210, and the [$^2H_2$]formaldehyde hydrazone was monitored at *m*/*z* 212. The ratio of M/M + 2 (*m*/*z* 210/212) was used as an estimate of the apparent $^D(V/K)$ for the dealkylation reaction. (ii) An intramolecular approach was used with deuterium-labeled **1** and **4**, with the methoxy group substituted with two deuteriums ($-OCHD_2$). The ratio [2(M + 2)/(M + 1)] (*m*/*z* 212/211, from integration of selected ion monitoring chromatograms) was used as an estimate of the apparent intrinsic ^Dk for the *O*-dealkylation reaction.

Kinetic Modeling. The results of pre-steady-state kinetic experiments were fit using the program DynaFit (*54*), which is based in part upon KINSIM and FITSIM methods (*55*−*57*) but has several advantages in terms of speed and diversity. The program was kindly provided by Dr. P. Kuzmic (University of Wisconsin, Madison, WI) and run on a Macintosh G3 computer (Apple Computer, Cupertino, CA). The program allows for reiterative fitting of rate and equilibrium constants. Typical files are included as Supporting Information.

RESULTS AND DISCUSSION

Effects of Substrate Alterations on Oxidation Rates. A series of phenacetin analogues were prepared and examined as substrates (Table 1). The substitutions made would not be expected to alter the oxidation−reduction potential (*58*) and influence any possible trend to a 1-electron-transfer mechanism (*12*), and we found that the potentials estimated by cyclic voltammetry were all nearly identical (results not shown). Therefore, we would expect any variability in oxidation to be due to changes in the interaction of substituents with the enzyme. All of the compounds yielded both the phenols (from *O*-dealkylation) and the acetols (Scheme 2). The identities of the acetols were verified by comparisons (HPLC, MS) with standard compounds, which were prepared by the described syntheses.

Substitution of the *O*-ethyl group of phenacetin with a methyl (**1**) did not dramatically change the *O*-dealkylation rate but lowered the rate of acetol formation (Table 2, Figure 1). Substitution with an (*O*-)isopropyl group (**2**) decreased the *O*-dealkylation rate; a low rate of hydroxylation of a methyl group of the isopropyl moiety was also detected (k_{cat} 0.045 min^{-1}). The remaining compounds (**3**, **4**, **5**), with bulkier *N*-acyl moieties, had significantly higher rates of both *O*-dealkylation and acetol formation. With **3** and **5**, higher K_m values were obtained. With **4**, a high K_m was measured

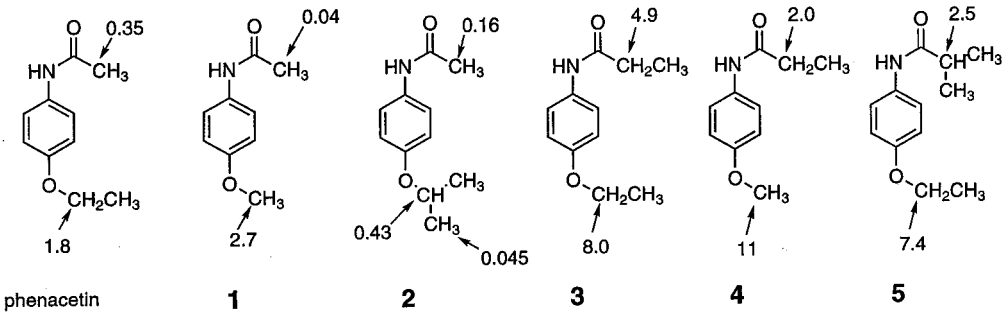

FIGURE 1: Rates of oxidation of substrates by (wild-type) P450 1A2. k_{cat} values for oxidations in individual reactions are shown (min^{-1}) (values from Table 2).

for acetol formation, compared to the lower value (15 μM) typical of phenacetin and substrates **1** and **2**.[6] The ratio of *O*-dealkylation to acetol formation, based on enzyme efficiencies (k_{cat}/K_m), varied from near unity (**2**) to 50 (**1**, **4**).

NADPH oxidation rates were measured with each substrate (200 μM concentrations) and were all in the range of 31−37 min^{-1}. With **3** and **4** the coupling efficiency of utilization of electrons from NADPH was much better (22% and 38%, respectively) than with phenacetin or any of the other substrates (1−8%), due to the higher rates of product formation.

We had previously selected P450 1A2 mutants from randomized libraries and found several with elevated catalytic activity, as well as less active mutants (*12*, *27*). Two mutants were examined with **4**, which had the highest *O*-dealkylation activity with wild-type P450 1A2 (Table 2, Figure 1). The *O*-dealkylation rate (at a 500 μM concentration of **4**) was 22 min^{-1}, which is considerably higher than the rate of *O*-dealkylation of the classical substrate phenacetin by wild-type P450 1A2 (k_{cat} 1.8 min^{-1}, Table 2). However, acetol formation (from **4**) was at the same rate as with wild-type P450 1A2 (1.4 min^{-1}). P450 D320A, a low activity mutant (*12*, *27*), showed low rates for both reactions with **4** (1.3 min^{-1} for *O*-deethylation, 0.06 min^{-1} for acetol formation).

The effects of modification of the prototype substrate phenacetin may be summarized: Increasing the size of the acyl group from two to four carbons had the effect of increasing rates of oxidations at both sites (e.g., compare substrates **3**, **4**, and **5** with phenacetin, **1**, and **2**, Figure 1). The increased acetol formation with **3**, **4**, and **5** was associated with an increased K_m (Table 2). The addition of more bulk in the acyl group (>propionamide) did not improve the rate of acetol formation (**5**). The substitution of a methyl vs ethyl group at the ether site did not influence rates of either reaction very much (Figure 1, Table 2); expanding the size of the substitutent to an isopropyl lowered the rate (**2**). Thus **4** appears to be the optimal *p*-alkoxyacylanilide within this set and was utilized in several further comparisons.

Binding Constants of Substrates and Products for P450 1A2. Human P450 1A2 (and also the E225I and D320A mutants) is isolated predominantly in the high-spin state (*12*, *47*) and are not amenable to some of the typical P450 spectral binding analysis methods, e.g., based on spin-state perturbation. We have used an approach to estimating affinity (K_s) based upon the change of P450 1A2 intrinsic fluorescence (Trp) upon binding of ligand (*63*), which has yielded similar binding parameters as UV−visible spin-state titration with rabbit P450 1A2 (*12*). Previously, we estimated K_s values of 31 ± 2, 24 ± 2, and 39 ± 5 μM for the binding of acetaminophen (**6**, *O*-deethylation product of phenacetin) to wild-type P450 1A2 and the E225I and D320A mutants, respectively (*12*).

The same fluorescence titration approach (with correction for inner filter effects) was used to estimate K_d for binding of the substrates to wild-type P450 1A2, yielding estimates in the range of 20−25 μM for all except **2**, which was 40 (±2) μM. A titration of wild-type P450 1A2 with **9**, the acetol product of **1**, yielded a K_s of 23 (±4) μM. As discussed later, these binding parameters all reflect binding of a nature that perturbs fluorescence, which may not be indicative of that required for substrate oxidation or competition. The changes in K_m (Table 2) are not interpreted in terms of only these binding constants, which are $\leq K_m$.

Noncompetitive Kinetic Deuterium Isotope Effects. Methacetin (**1**) has some useful features in the study of deuterium isotope effects on *O*-dealkylation, e.g., the lack of prochirality in *O*-dealkylation experiments. As in our previous work with phenacetin *O*-deethylation (*12*), the noncompetitive kinetic deuterium isotope effects were relatively low (1.3−3.2) (Table 3), particularly in comparison to the values of ∼14 measured for acetol formation with phenacetin (*12*). The order of the isotope effects followed the rates, i.e., E225I > wild-type > D320A, especially $^{D}(V/K)$ (Table 3), a trend that had seemed to be occurring with phenacetin but was not statistically significant (*12*).

In the previous work with phenacetin (*12*), lowering rates of *O*-deethylation by deuterium substitution did not increase acetol formation. However, increased acetol formation with deuterated **1** was seen and is interpreted as evidence for "metabolic switching", in which the commitment of an enzyme intermediate to product formation allows some turning of the substrate for the iron−oxygen complex to encounter an alternate site when oxidation of the normal site becomes less favorable (*64*). Apparently the binding of **1** is such that this movement is possible.

Similar noncompetitive kinetic deuterium isotope effects were measured for the *O*-deisopropylation of **2** by wild-type P450 1A2, $^{D}V = 1.9 \pm 0.1$ and $^{D}(V/K) = 1.6 \pm 0.3$. These isotope effects can be contrasted with $^{D}V = 5.0 \pm 0.8$ for the slower ($k_{cat} \sim 0.045$ min^{-1} for d_0) hydroxylation of the methyl group of the isopropyl moiety, i.e., position adjacent to that for which the lower isotope effects are measured

[6] The existence of different K_m values for alternate products formed from a single substrate by a recombinant enzyme has been observed earlier with other P450s (*59*−*62*).

Table 3: Intermolecular Isotope Effects on *O*-Dealkylation and Acetyl Hydroxylation of Methacetin (**1**) by P450 1A2 Mutants

1A2	methacetin d_n ($-OCH_3$)	*O*-demethylation (acetaminophen formation) k_{cat} (min^{-1})	K_m (μM)	^DV	$^D(V/K)$	acetol formation k_{cat} (min^{-1})	K_m (μM)	^DV	$^D(V/K)$
wild type	d_0	2.7 ± 0.1	28 ± 3			0.039 ± 0.010	20 ± 7		
	d_3	0.94 ± 0.02	23 ± 2	2.9 ± 0.1	2.4 ± 0.4	0.10 ± 0.01	24 ± 4	0.38 ± 0.10	0.46 ± 0.21
E2251	d_0	9.6 ± 0.3	22 ± 2			0.12 ± 0.01	14 ± 6		
	d_3	3.0 ± 0.1	21 ± 2	3.2 ± 0.1	3.1 ± 0.4	0.29 ± 0.02	13 ± 3	0.42 ± 0.05	0.38 ± 0.19
D320A	d_0	0.073 ± 0.005	310 ± 40			not determined[a]			
	d_3	0.055 ± 0.006	330 ± 70	1.3 ± 0.2	1.4 ± 0.4				

[a] The amount of product formed was too low to accurately determine the kinetic parameters under these reaction conditions.

Table 4: Competitive Kinetic Deuterium Isotope Effects for *p*-Alkoxyacylanilide *O*-Dealkylation by P450 1A2

substrate	P450 1A2	intermolecular $^D(V/K)$	intramolecular $^D(V/K)$
methacetin (**1**) (d_2)	wild type	3.1 ± 0.2	5.4 ± 0.3
	E225I	3.3 ± 0.4	6.8 ± 0.5
N-(4-methoxyphenyl)-propionamide (**4**) (d_2)	wild type	3.1 ± 0.2	6.6 ± 0.3
	E225I	3.1 ± 0.1	7.0 ± 0.1

(Figure 1). The noncompetitive isotope effects for *O*-demethylation of **4** by wild-type P450 1A2 were $^DV = 2.5 \pm 0.2$ and $^D(V/K) = 2.7 \pm 0.5$.

Competitive Kinetic Deuterium Isotope Effects. The intermolecular kinetic deuterium isotope effects were measured by MS of (derivatized) formaldehyde released from the *O*-demethylation of **1** or **4** (Table 4). The observed values are only slightly higher than the noncompetitive $^D(V/K)$ values (Table 3 and above text).

The intramolecular isotope effects, measured by the MS analysis of formaldehyde formed from d_2-methyl substrates, were in the range of 5.4−7.0 for wild-type P450 1A2 and the mutant E225I (Table 4). These intramolecular isotope effects should, in principle, approximate the intrinsic isotope effect for the reaction (i.e., ^Dk, the isotope effect on the isotopically sensitive step). These values are higher than the noncompetitive or competitive intermolecular isotope effects and suggest attenuation of the isotopically sensitive steps by other steps, i.e., that the isotopically sensitive step is not the only step controlling the *O*-dealkylation rates.

Kinetic Modeling: General Considerations. The results obtained in this work yielded an extensive set of steady-state results with several related enzymes and substrates. These are considered in systems using the program DYNAFIT (*54*), similar to the KINSIM and FITSIM programs (*55*, *56*) that we have used previously with P450 (*65*), which can be used to simulate results and also to fit data with values of parameters that are most appropriate mathematically. A general approach in kinetic modeling is to use the simplest possible models first, because even then the number of equations usually already exceeds the number of known parameters and unique solutions may not be possible.

The mechanism shown in Scheme 1 was used. Reaction 5 represents all steps between the $(FeO_2)^+$ entity and a form of P450 capable of directly oxidizing the substrate; step 6 ("oxygenation") can represent any alternative chemical set of reactions leading to the product P. Step 7 includes any rate-limiting step following formation of the P450-product complex, EP. The mechanism is applied to each product individually, i.e., phenol or acetol. Accounting for the formation of H_2O_2 and H_2O is critical in this system. Step 8 represents the conversion of $(FeO_2)^+$ to H_2O_2 (alternatively, H_2O_2 could be formed from $Fe^{2+}O_2$; such a possibility has not been included). Formation of H_2O is presumed to occur only from reduction of the species labeled $(FeO)^{3+}$ in Scheme 1 (*66*). H_2O formation becomes a critical point in some considerations, and a deficiency in all work with P450s is the lack of ability to measure this directly [i.e., H_2O formation is only estimated by stoichiometry differences (*66*)].

Table 5: Rate Constants Used for Modeling Phenacetin Oxidations

rate constants[a] (min^{-1} or $min^{-1}\ \mu M^{-1}$)	rate constants[a] (min^{-1} or $min^{-1}\ \mu M^{-1}$)
$k_1 = 6000$; $k_{-1} = 120000$	k_6 = variable
$k_2 = 700$	$k_7 = 660$; $k_{-7} = 6000$
$k_3 = 6000$; $k_{-3} = 6$	$k_8 = 50$
$k_4 = 700$	$k_9 = 50$
$k_5 = 110$	

[a] See Scheme 1. First-order rate constants (k_{-1}, k_2, k_{-3}, k_4, k_5, k_6, k_7, k_8, k_9) are in min^{-1}, and second-order rate constants (k_1, k_3, k_{-7}) are in $min^{-1}\ \mu M^{-1}$.

To simplify the mechanistic considerations, steps 2, 4, 5, 6, 8, and 9 of Scheme 1 are written as being irreversible. Steps 5, 6, and 9 probably are irreversible; the other steps in this group are strongly committed in the forward direction under the experimental conditions, and modeling efforts indicated that fits required very slow back-reactions. All second-order reactions were set at $6 \times 10^9\ M^{-1}\ min^{-1}$ ($10^8\ M^{-1}\ s^{-1}$), a reasonable rate for diffusion-controlled encounters between large and small molecules.

Some other pieces of available information were used to direct the efforts (Table 5). The initial K_d for step 1 (substrate binding, Scheme 1) was set near that estimated by fluorescence quenching titrations (although any assumptions used here must have caveats, as discussed later). Previously we experimentally measured the rate of step 2 (reduction) as $700\ min^{-1}$ (*11*, *12*) and used this value. In our initial trials, we used the same rate for step 4 (introduction of the second electron). Step 3, O_2 binding, is generally considered to have a low K_d, as judged by the ready oxidation of ferrous P450 (*67*), and subsequent fitting was very consistent with this view [the k_{off} rate for O_2 in bacterial P450 101 is reported at $2.7\ s^{-1}$ and the K_d as 3×10^{-8} M (*68*)]. Finally, steady-state rates of formation of H_2O_2 and H_2O have been estimated under these experimental conditions, e.g., 11 and $12\ min^{-1}$, respectively, for wild-type P450 1A2 during phenacetin oxidation (*12*) and were used as minimum rates to begin the fitting procedure. Separate kinetic trials were done with the mechanism in Scheme 1 and sets of parameters to determine if the rates of H_2O_2 and H_2O formation were consistent with

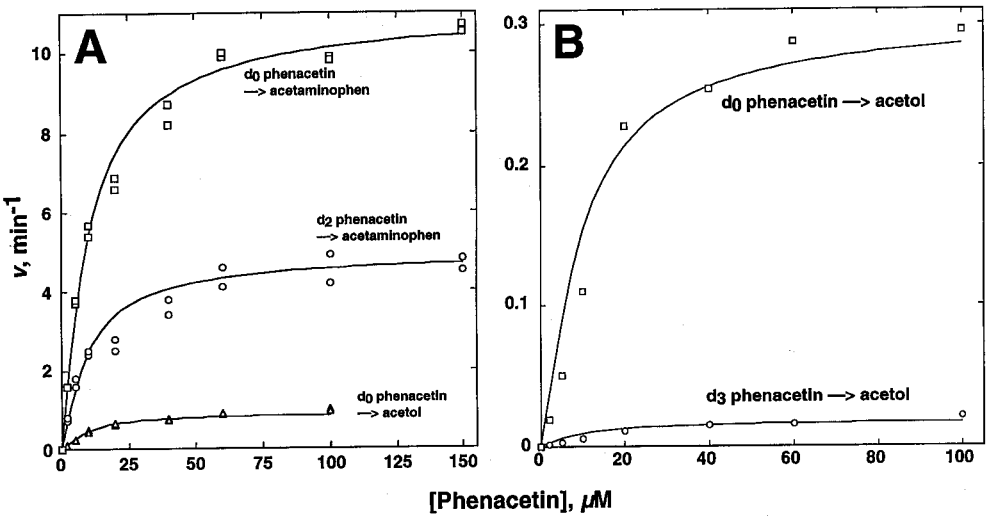

FIGURE 2: Fits to steady-state kinetic data for phenacetin oxidation by P450 1A2. (A) Mutant E225I. The points shown were measured experimentally for *O*-deethylation (□, d_0 substrate; ○, 1,1-d_2-ethyl substrate) and acetol formation (△, d_0 phenacetin). The mechanism and rate constants in Scheme 1 and Table 5 were used in all three of the traces (solid lines): $k_6 = 110$ min^{-1} (□), $k_6 = 40$ min^{-1} (○), and $k_6 = 6.5$ min^{-1} (△). (B) Wild-type P450 1A2. Experimental points are shown for the d_0 substrate (□) and 1,1-d_2-ethyl substrate (○). The mechanism and rate constants in Scheme 1 and Table 5 were used in both traces (solid lines): $k_6 = 2.2$ min^{-1} (□) and $k_6 = 0.12$ min^{-1} (○).

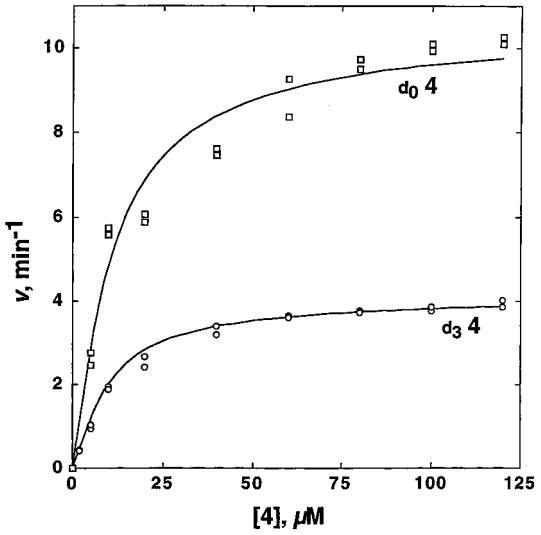

FIGURE 3: Fits to steady-state kinetic data for *O*-demethylation of **4** by wild-type P450 1A2. Experimental points are shown for the d_0 (□) and *O*-methyl d_3 (○) substrates. The mechanism and rate constants in Scheme 1 and Table 5 were used, except that k_{-1} was adjusted to 1.3×10^5 min^{-1} ($K_d = 22$ μM). Solid lines are simulated fits with $k_6 = 103$ min^{-1} (□) and 35 min^{-1} (○).

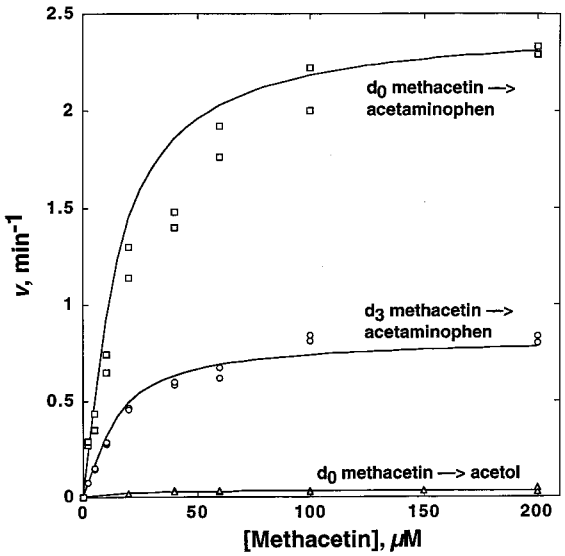

FIGURE 4: Fits to steady-state kinetic data for methacetin (**1**) *O*-demethylation by wild-type P450 1A2. Experimental points are shown for the d_0 (□) and *O*-methyl d_3 (○) substrates. The mechanism and rate constants in Scheme 1 and Table 5 were used in both cases, except that k_{-1} was adjusted to 1.8×10^5 min^{-1} ($K_d = 29$ μM). Solid lines are simulated fits with $k_6 = 18$ min^{-1} (□) and 6 min^{-1} (○).

experimental values (product vs time curves, which were also developed using the DYNAFIT program).

The major approach used was fitting of plots of rates of steady-state product formation (v) vs substrate concentration (S) (Figures 2−4). The systems were most sensitive to k_5 and k_6. Intuitively, it seems reasonable that k_5 should be rather invariant of the substrate, or at least deuterium substitution, and we sought a single rate (for k_5) that could be utilized in all of the reactions with each P450.

Kinetic Modeling: Wild-Type P450 1A2 and E225I Mutant. The mechanism in Scheme 1 was used to model the results collected on the oxidation of the substrates (Table 1) by wild-type P450 1A2 and the E225I mutant, using the general constraints described above. The E225I mutant was originally selected from an activity screen with a randomized library (in the "substrate recognition sequence" 2 region) based on its high catalytic activity (*27*); sequence alignment suggests a position in the F helix. The availability of a broad collection of rates of product formation with the different substrates (Figure 1, Table 2) and isotopic derivatives (Table 3) allowed the exploration of the origin of the basis of the parameters k_{cat} and K_m and the kinetic hydrogen isotope effects. The values of the rate constants used for phenacetin oxidations are shown in Table 5. Slight adjustments were made for k_{-1} (substrate off-rate) for other substrates, as indicated in the figure legends. Some of the fits for oxidations of phenacetin, **1**, and **4** are shown in Figures 2−4.

Several comments about the fitting are in order. The set of constants presented in Table 5 could be used for all of the reactions considered and did not require adjustment. Thus, the results of the simulation analysis are consistent with (but

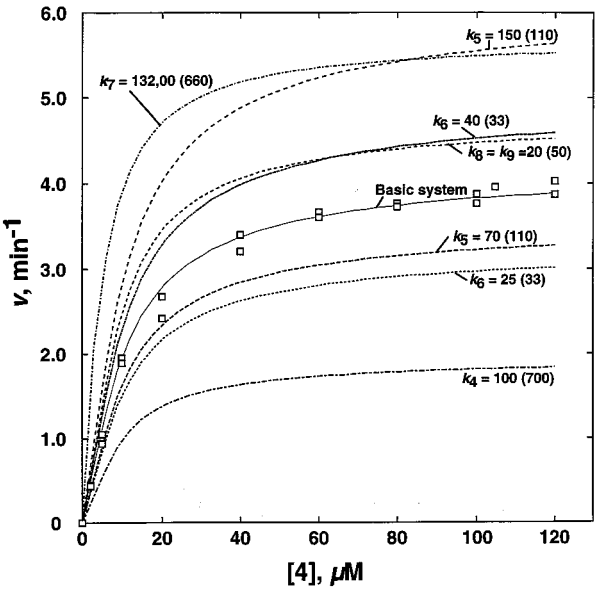

FIGURE 5: Effects of changes in rate constants on fits to *O*-demethylation of d_3-**4** by wild-type P450 1A2. The basic mechanism and individual rate constants are shown in Scheme 1 and Table 5 ($k_6 = 33$ min^{-1}) and were used to fit the data points (□) ("basic system"). Traces drawn with modifications of single constants are shown on the figure, with the original rate constant (from the basic system) shown in parentheses.

do not necessarily prove) the view that the catalytic mechanism can be described by a series of steps with finite rates and changes only in one or a few steps. k_6, the step (product formation) that should be isotopically sensitive, was the only constant that needed to be varied to fit most of the plots, including those with deuterium substitution. The intrinsic isotope effect predicted in these fits was generally ~2−3 for *O*-dealkylation (Figures 2A, 3, 4) and almost 20 for acetol formation (Figure 2B). The fact that these *O*-dealkylation ^{D}k estimates are less than some of the intramolecular competitive isotope effects (Table 4) may be indicative of an additional step hidden in the mechanism of Scheme 1 that makes a contribution.

A major limitation on the models is the need to produce H_2O_2 and H_2O at rates consistent with those estimated experimentally. Use of the mechanism shown in Scheme 1 with $k_6 = 110$ min^{-1} yielded an initial rate of H_2O_2 production of 14 min^{-1} in the case of the E225I mutant and (d_0) phenacetin (Figure 2) [cf. experimental 11 (±1) min^{-1} in the presence of phenacetin and 15 (±1) min^{-1} in the absence (*12*)].

Some indication of the dependence of the fits on individual rate constants is shown in Figure 5, with one set of experimental data used as an example (*O*-demethylation of d_3-**4** by wild-type P450 1A2). A change in k_6 (product formation, which can be considered the step most sensitive to changes in terms of losing the curve fits) had dramatic effects. The good fit shown with $k_6 = 33$ min^{-1} was clearly lost when k_6 was set at either 25 or 40 min^{-1}. k_5, the step associated with activation of $(FeO_2)^+$ to an oxygenating complex (FeO^{3+}?), gave good fits when set at 90−110 min^{-1}, but values of 70 or 150 min^{-1} were not acceptable. k_4, the rate of addition of the second electron into the P450 system, was originally set at 700 min^{-1} and could be lowered to ~350 min^{-1} with an acceptable fit. This step is of interest in that it is often proposed to be the reason for the enhancement of other P450 oxidations by cytochrome b_5 (*15*, *16*). Lowering k_4 to 100 min^{-1} clearly did not yield an acceptable fit (Figure 5).

The ratios of k_{-1}/k_1 (substrate binding) used in these models are similar to the K_d values estimated by fluorescence titrations with substrates (~20 μM). One issue in the fitting is that the use of k_7 values (product off-rate, plus any associated steps) that yielded k_7/k_{-7} ratios near the expected K_d values estimated by the fluorescence titrations with the phenolic products gave poor fits, with unrealistically low K_m estimates (Figure 5). Adjustments to k_{-1} yielded acceptable fits only when the ratio k_7/k_{-7} was much less than k_{-1}/k_1 (i.e., $K_{d,product} < K_{d,substrate}$). Because P in the mechanism (Scheme 1) is a collection of at least two products (phenol, acetol), the mechanism does not distinguish between them, and the possibility can be considered that the acetol has high affinity for ferric P450 1A2. This possibility was examined in a direct fluorescence titration. The apparent K_d was 23 (±4) μM for **10**, the acetol derived from phenacetin, similar to that estimated for acetaminophen. The possibility exists that the estimated K_d values do not accurately reflect the affinity of the product at the end of the reaction cycle.

The same mechanism could be used to model the results of oxidation to either phenols or acetols, with good fits resulting from changing only k_6, the oxygenation step (Figures 2, 4). The mechanism and the rate constants used do not imply that these are unique solutions for wild-type P450 1A2 and the E225I mutant. However, they are viewed as reasonable values that can satisfy several criteria, including isotope effects and rates of formation of reduced O_2 species as well as v vs S plots. The model describes a system in which changes in k_4, k_5, k_6, k_8, and k_9 can all have major effects on rates of product formation.

Kinetic Modeling: D320A Mutant. The D320A mutant is of interest because of its low activity toward a number of substrates (*12*, *27*). The mutant is not impaired in its ability to bind (thiol-liganded) heme or its rate of reduction to the ferrous form (*12*). This mutant is analogous to the rat P450 1A2 E318A mutant (and other Glu318 mutants) studied extensively by Shimizu and his associates (*28*−*30*, *69*−*71*) and to (bacterial) P450 101 Asp 251 mutants (*68*, *72*, *73*).[7]

This mutant, in contrast to mutant E225I with enhanced activity, presented a number of problems in transposing the mechanism and kinetic constants used for wild-type P450 1A2. One problem is the high K_m values observed for *O*-dealkylation of either phenacetin (~300 μM) (*12*) or **1** (Table 5). The K_d for phenacetin estimated from fluorese-

[7] In bacterial P450 101, Asp251 is considered to be part of a distal charge relay system with an H-bonding network including basic residues. Substitution at Asp251 does not affect camphor or oxygen binding, reduction, or autoxidation rates but does lower the rate of catalysis 100-fold (*68*, *72*). Krainev et al. (*69*) concluded that interactions between rat P450 1A2 Glu318 with other amino acids were necessary to shape the heme pocket, and the E318A mutant showed altered affinity for several heme ligands. Nakano et al. (*70*) later reported that the E318A substitution markedly facilitated nonenzymatic reduction of the ferric−NO complex of this P450. Thus, work with these analogous mutants suggests a role in ligand affinity and proton and electron relay in the active site. Interestingly, Hiroya et al. (*28*) reported that the rat P450 1A2 substitution E318A attenuated NADPH oxidation, as well as oxidation of the substrate CH_3OH, and no H_2O_2 was formed. In apparent contrast, our work with the (human) P450 1A2 D320A mutant showed increased NADPH oxidation and H_2O_2 formation relative to the wild-type enzyme (*12*).

cence quenching was ~20 μM, as in the case of wild-type P450 1A2 (*12*).

An issue with the D320A mutant is that the function of such acidic residues near a Thr in the heme distal region is considered to be part of a charge relay involved in O−O bond scission (*68*, *74*, *75*). If this were the only change elicited by the D320A substitution, attenuation of only k_5 (O−O bond scission) might be expected to be sufficient to fit the experimental results. However, reducing k_5 to a value consonant with formation of phenol products from phenacetin (*12*) or **1** (Table 5) had the effect of eliminating H_2O formation, as might be expected. One possibility is that H_2O is not actually formed and the H_2O_2 estimates are underestimated. However, this possibility seems unlikely in the face of evidence from other P450 systems that pathways for H_2O formation other than electron and proton input into a monooxygen complex are not known ($O_2^{\bullet-}$ would not accumulate and would yield H_2O_2; Scheme 1). We could fit the experimental results (with phenacetin or **1**) but doing so required changes in both k_{-1} (substrate off-rate) and k_6 (oxygenation), to satisfy the issue of H_2O formation as well as the v vs S fit.[8] The physical interpretations would be that substrate binding is altered and substrate oxidation is the most affected step. Attenuation of only the O−O bond-breaking step is not indicated. We previously reported that the steady-state levels of a spectrally detectable iron−oxygen complex were lower in the D320A mutant than in the wild-type enzyme or the E225I mutant (*12*). However, we are not certain what specific complex this spectrum represents. Thus, substitution of a single residue in a P450 appears to yield effects on a number of parameters, some of which may be interrelated. The complexity of site-directed mutagenesis results is often greater than can be accommodated by simple models, even for single mutations.

Conclusions. A long-standing problem in mechanistic studies with P450 1A2 enzymes has been the low rates of reactions (*12*, *23*, *28*, *29*). Modifications in the prototype substrate phenacetin were introduced, and the coupling efficiency (products formed/NADPH oxidized) was increased to 38%. Use of a mutant enzyme with enhanced catalytic activity (E225I) raised the overall rate of product formation from **4** to 23 min^{-1}.

Kinetic models were used to address the issue of which individual steps of the P450 1A2 kinetic cycle are rate-limiting in steady-state catalysis. A simplified model was developed which could be used to fit the available results obtained with wild-type P450 1A2, both for phenol and for acetol formation and also satisfying the need to account for uncoupling to yield H_2O_2 and H_2O. Varying only the product formation step, k_6 (Scheme 1), allowed fitting of most systems (with slight changes of the substrate off-rate k_{-1} for different substrates), and the isotope effects could be satisfied with these changes. k_6 was the slowest step in most cases. However, k_6 was always considerably higher than k_{cat}, because of the need to introduce rates of ~50 min^{-1} for k_8 and k_9, the reactions leading to H_2O_2 and H_2O. The traces shown in Figure 5 demonstrate the sensitivity of the system to rates of multiple individual steps. Although k_6 (product formation) is the slowest rate constant in the system, <2-fold changes in rates of steps k_4, k_5, k_8, and k_9 can all produce considerable alterations in the fits. The effect produced by changing k_4 (second 1-electron reduction) would also be expected with k_2 (first 1-electron reduction), particularly with substrates with higher rates. k_6 (product formation) alone can account for the isotope effects, although this may be an oversimplification.

One aspect of the modeling that remains to be examined further is the dependence of K_m on individual rate constants. The K_m, as expected, can be changed by altering k_{-1} or k_7 (substrate and product off-rates) of Scheme 1 (e.g., Figure 5). However, K_m is also sensitive to changes in k_8 and k_9, the rates of uncoupled O_2 reduction. In Figure 5, the fit to the line denoted "$k_8 = k_9 = 20$ min^{-1}" yields $k_{cat} = 4.9$ min^{-1} and $K_m = 9.4$ μM, which can be compared to the values of $k_{cat} = 4.5$ min^{-1} and $K_m = 15$ ($\pm$1) μM fit to the experimental data ("basic system", which fits to $k_8 = k_9 = 50$ min^{-1}). Exactly which microscopic rate constants can influence K_m is an issue that requires further consideration with this and other P450 enzymes. We have previously developed the P450 2E1 kinetic model with a rate-determining step (for some substrates) to account for the influence of deuteration on K_m (*53*, *65*). In the system analyzed here, the rate constants for all of the individual steps are faster than k_{cat}, because of their similarity. The balance of rate constants proposed here (Scheme 1), if this model is applicable to other P450s, should yield situations in which changes in any of several steps may have important effects (Figure 5). If this view is valid, then several steps in the catalytic cycle have similar transition state barrier heights and influence which reactions proceed.

ACKNOWLEDGMENT

We thank H. Cai for recording NMR spectra and for assistance with literature searches, I. H. Hanna for helpful discussions, and B. Fox and L. Manier for technical assistance with MS.

SUPPORTING INFORMATION AVAILABLE

Schemes showing the DYNAFIT reaction mechanism, differential equations, and the sample DYNAFIT operating file used for Figure 5. This information is available free of charge via the Internet at http://pubs.acs.org.

REFERENCES

1. Palmer, G., and Reedijk, J. (1992) *J. Biol. Chem. 267*, 665−677.
2. Northrop, D. B. (1975) *Biochemistry 14*, 2644−2651.
3. Northrop, D. B. (1982) *Methods Enzymol. 87*, 607−625.
4. Guengerich, F. P. (1991) *J. Biol. Chem. 266*, 10019−10022.
5. Guengerich, F. P. (1995) in *Cytochrome P450* (Ortiz de Montellano, P. R., Ed.) pp 473−535, Plenum Press, New York.

[8] One possibility we considered was that Asp320 has a role in a process that follows oxidation of the substrate, e.g., cleavage of the presumed hemiacetal product. Such a mechanism may have some precedent in our work on ethanol oxidation by P450 2E1, in which a rate-limiting step follows product formation (*65*). In studies with wild-type P450 1A2 and the E225I mutant, we did not detect a burst phase for product formation in the oxidation of phenacetin to either the phenol or acetol (*12*), arguing against a rate-limiting step at this point in the catalytic cycle. However, it is conceivable that an important post-product formation step might have been attenuated by the substitution at Asp320. Adding a rapid step following k_6 (product formation) to the mechanism of Scheme 1 yielded satisfactory fits for wild-type P450 1A2, as expected (k > 300 min^{-1}). However, adjusting only this added step did not yield satisfactory fits to the data for D320A without adjustments of other parameters.

6. White, R. E., and Coon, M. J. (1980) *Annu. Rev. Biochem. 49*, 315−356.
7. Ortiz de Montellano, P. R. (1986) in *Cytochrome P-450* (Ortiz de Montellano, P. R., Ed.) pp 217−271, Plenum Press, New York.
8. McMurry, T. J., and Groves, J. T. (1986) in *Cytochrome P-450* (Ortiz de Montellano, P. R., Ed.) pp 1−28, Plenum Press, New York.
9. Ortiz de Montellano, P. R. (1995) in *Cytochrome P450: Structure, Mechanism, and Biochemistry* (Ortiz de Montellano, P. R., Ed.) pp 245−303, Plenum Press, New York.
10. Vaz, A. D. N., Pernecky, S. J., Raner, G. M., and Coon, M. J. (1996) *Proc. Natl. Acad. Sci. U.S.A. 93*, 4644−4648.
11. Guengerich, F. P., and Johnson, W. W. (1997) *Biochemistry 36*, 14741−14750.
12. Yun, C.-H., Miller, G. P., and Guengerich, F. P. (2000) *Biochemistry 39*, 11319−11329.
13. Ullrich, V. (1969) *Hoppe-Seyler's Z. Physiol. Chem. 350*, 357−365.
14. Hildebrandt, A., and Estabrook, R. W. (1971) *Arch. Biochem. Biophys. 143*, 66−79.
15. Noshiro, M., Ullrich, V., and Omura, T. (1981) *Eur. J. Biochem. 116*, 521−526.
16. Pompon, D., and Coon, M. J. (1984) *J. Biol. Chem. 259*, 15377−15385.
17. Groves, J. T., McClusky, G. A., White, R. E., and Coon, M. J. (1978) *Biochem. Biophys. Res. Commun. 81*, 154−160.
18. Björkhem, I. (1973) *Biochem. Biophys. Res. Commun. 50*, 581−587.
19. Lu, A. Y. H., Harada, N., and Miwa, G. T. (1984) *Xenobiotica 14*, 19−26.
20. Guengerich, F. P. (1987) *J. Biol. Chem. 262*, 8459−8462.
21. Guengerich, F. P., Peterson, L. A., and Böcker, R. H. (1988) *J. Biol. Chem. 263*, 8176−8183.
22. Distlerath, L. M., Reilly, P. E. B., Martin, M. V., Davis, G. G., Wilkinson, G. R., and Guengerich, F. P. (1985) *J. Biol. Chem. 260*, 9057−9067.
23. Butler, M. A., Iwasaki, M., Guengerich, F. P., and Kadlubar, F. F. (1989) *Proc. Natl. Acad. Sci. U.S.A. 86*, 7696−7700.
24. Shimada, T., Iwasaki, M., Martin, M. V., and Guengerich, F. P. (1989) *Cancer Res. 49*, 3218−3228.
25. Turesky, R. J., Constable, A., Richoz, J., Vargu, N., Markovic, J., Martin, M. V., and Guengerich, F. P. (1998) *Chem. Res. Toxicol. 11*, 925−936.
26. Gotoh, O. (1992) *J. Biol. Chem. 267*, 83−90.
27. Parikh, A., Josephy, P. D., and Guengerich, F. P. (1999) *Biochemistry 38*, 5283−5289.
28. Hiroya, K., Ishigooka, M., Shimizu, T., and Hatano, M. (1992) *FASEB J. 6*, 749−751.
29. Furuya, H., Shimizu, T., Hirano, K., Hatano, M., Fujii-Kuriyama, Y., Raag, R., and Poulos, T. L. (1989) *Biochemistry 28*, 6848−6857.
30. Shimizu, T., Sadeque, A. J. M., Sadeque, G. N., Hatano, M., and Fujii-Kuriyama, Y. (1991) *Biochemistry 30*, 1490−1496.
31. Allen, C. F. H., and Gates, J. W., Jr. (1955) *Org. Synth. 3*, 140−141.
32. Shapiro, S. L., Rose, I. M., and Freedman, L. (1959) *J. Am. Chem. Soc. 81*, 6322−6329.
33. Garland, W. A., Nelson, S. D., and Sasame, H. A. (1976) *Biochem. Biophys. Res. Commun. 72*, 539−545.
34. Sundberg, R. J., and Smith, R. H. (1971) *J. Org. Chem. 36*, 267−270.
35. Hill, A. J., and Rabinowitz, I. (1926) *J. Am. Chem. Soc. 48*, 732−737.
36. Hill, A. J., and Cox, M. V. (1926) *J. Am. Chem. Soc. 48*, 3214−3219.
37. De Feo, R. J., and Strickler, P. D. (1963) *J. Org. Chem. 28*, 2915−2917.
38. Bell, M. R. (1974) U.S. Patent US 3819637.
39. Bell, M. R. (1975) *Chem. Abstr. 81*, 120496.
40. Joshi, B. P., and Hosangadi, B. D. (1978) *Ind. J. Chem., Sect. B 16B*, 1067−1072.
41. Societe d'Etudes Scientifiques et Industrielles de l'Ile-de-France (1962) French Patent FR M2307.
42. (1964) *Chem. Abstr. 60*, 15780.
43. Smith, G. E., and Griffiths, L. A. (2000) *Xenobiotica 4*, 477−487.
44. Brand, K., and Priesner, R. (1952) *Arch. Pharmacol. 285*, 26−34.
45. Elbs, K. (1911) *J. Prakt. Chem. 83*, 1−21.
46. Weidner, J. J., Weintraub, P. M., Schnettler, R. A., and Peet, N. P. (1997) *Tetrahedron 53*, 6303−6312.
47. Sandhu, P., Guo, Z., Baba, T., Martin, M. V., Tukey, R. H., and Guengerich, F. P. (1994) *Arch. Biochem. Biophys. 309*, 168−177.
48. von Moltke, L. L., Greenblatt, D. J., Duan, S. X., Schmider, J., Kudchadker, L., Fogelman, S. M., Harmatz, J. S., and Shader, R. I. (1996) *Psychopharmacology 128*, 398−407.
49. Shen, A. L., Porter, T. D., Wilson, T. E., and Kasper, C. B. (1989) *J. Biol. Chem. 264*, 7584−7589.
50. Hanna, I. H., Teiber, J. F., Kokones, K. L., and Hollenberg, P. F. (1998) *Arch. Biochem. Biophys. 350*, 324−332.
51. Guengerich, F., P. (1994) in *Principles and Methods of Toxicology* (Hayes, A., W., Ed.) pp 1259−1313, Raven Press, New York.
52. Shriner, R. L., Fuson, R. C., and Curtin, D. Y. (1965) in *The Systematic Identification of Organic Compounds*, pp 253−254, Wiley, New York.
53. Bell, L. C., and Guengerich, F. P. (1997) *J. Biol. Chem. 272*, 29643−29651.
54. Kuzmic, P. (1996) *Anal. Biochem. 237*, 260−273.
55. Barshop, B. A., Wrenn, R. F., and Frieden, C. (1983) *Anal. Biochem. 130*, 134−145.
56. Frieden, C. (1993) *Trends Biochem. Sci. 18*, 58−60.
57. Zimmerle, C. T., and Frieden, C. (1989) *Biochem. J. 258*, 381−387.
58. Miner, D. J., Rice, J. R., Riggin, R. M., and Kissinger, P. T. (1981) *Anal. Chem. 53*, 2258−2263.
59. Hosea, N. A., Miller, G. P., and Guengerich, F. P. (2000) *Biochemistry 39*, 5929−5939.
60. Maenpää, J., Hall, S. D., Ring, B. J., Strom, S. C., and Wrighton, S. A. (1998) *Pharmacogenetics 8*, 137−155.
61. Kerr, B. M., Thummel, K. E., Wurden, C. J., Klein, S. M., Kroetz, D. L., Gonzalez, F. J., and Levy, R. H. (1994) *Biochem. Pharmacol. 47*, 1969−1979.
62. Shou, M., Mei, Q., Ettore, M. W., Jr., Dai, R., Baillie, T. A., and Rushmore, T. H. (1999) *Biochem. J. 340*, 845−853.
63. Ehrenberg, M., Cronvall, E., and Rigler, R. (1971) *FEBS Lett. 18*, 199−203.
64. Miwa, G. T., and Lu, A. Y. H. (1987) *BioEssays 7*, 215−219.
65. Bell-Parikh, L. C., and Guengerich, F. P. (1999) *J. Biol. Chem. 274*, 23833−23840.
66. Gorsky, L. D., Koop, D. R., and Coon, M. J. (1984) *J. Biol. Chem. 259*, 6812−6817.
67. Oprian, D. D., Gorsky, L. D., and Coon, M. J. (1983) *J. Biol. Chem. 258*, 8684−8691.
68. Mueller, E. J., Loida, P. J., and Sligar, S. G. (1995) in *Cytochrome P450: Structure, Mechanism, and Biochemistry* (Ortiz de Montellano, P. R., Ed.) pp 83−124, Plenum Press, New York.
69. Krainev, A. G., Shimizu, T., Ishigooka, M., Hiroya, K., Hatano, M., and Fujii-Kuriyama, Y. (1991) *Biochemistry 30*, 11206−11211.
70. Nakano, R., Sato, H., Watanabe, A., Ito, O., and Shimizu, T. (1996) *J. Biol. Chem. 271*, 8570−8574.
71. Shimizu, T., Ito, O., Hatano, M., and Fujii-Kuriyama, Y. (1991) *Biochemistry 30*, 4659−4662.
72. Gerber, N. C., and Sligar, S. G. (1992) *J. Am. Chem. Soc. 114*, 8742−8743.
73. Vidakovic, M., Sligar, S. G., Li, H., and Poulos, T. L. (1998) *Biochemistry 37*, 9211−9219.
74. Poulos, T. L., and Raag, R. (1992) *FASEB J. 6*, 674−679.
75. Xiang, H., Tschirret-Guth, R. A., and Ortiz de Montellano, P. R. (2000) *J. Biol. Chem. 275*, 35999−36006.

BI002906N